Article

"Clickable" Organic Electrochemical Transistors

Gonzalo E. Fenoy,* Roger Hasler, Felice Quartinello, Waldemar A. Marmisollé, Christoph Lorenz, Omar Azzaroni,* Peter Bäuerle,* and Wolfgang Knoll*

Read Online

ACCESS | Metrics & More | Article Recommendations | Supporting Information

ABSTRACT: Interfacing the surface of an organic semiconductor with biological elements is a central quest when it comes to the development of efficient organic bioelectronic devices. Here, we present the first example of "clickable" organic electrochemical transistors (OECTs). The synthesis and characterization of an azide-derivatized EDOT monomer (azidomethyl-EDOT, EDOT-N$_3$) are reported, as well as its deposition on Au-interdigitated electrodes through electropolymerization to yield PEDOT-N$_3$-OECTs. The electropolymerization protocol allows for a straightforward and reliable tuning of the characteristics of the OECTs, yielding transistors with lower threshold voltages than PEDOT-based state-of-the-art devices and maximum transconductance voltage values close to 0 V, a key feature for the development of efficient organic bioelectronic devices. Subsequently, the azide moieties are employed to click alkyne-bearing molecules such as redox probes and biorecognition elements. The clicking of an alkyne-modified PEG$_4$-biotin allows for the use of the avidin−biotin interactions to efficiently generate bioconstructs with proteins and enzymes. In addition, a dibenzocyclooctyne-modified thrombin-specific HD22 aptamer is clicked on the PEDOT-N$_3$-OECTs, showing the application of the devices toward the development of organic transistors-based biosensors. Finally, the clicked OECTs preserve their electronic features after the different clicking procedures, demonstrating the stability and robustness of the fabricated transistors.
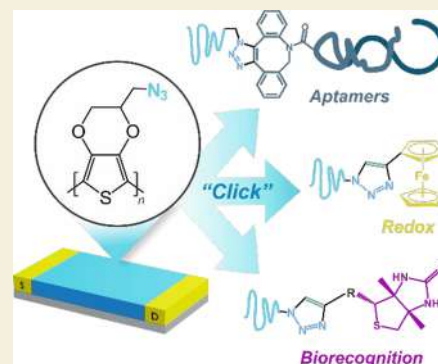
KEYWORDS: *organic electrochemical transistors, click chemistry, thrombin, biotin−avidin, organic bioelectronics*

INTRODUCTION

During the last two decades, the field of organic bioelectronics has appeared as a novel and innovative area where researchers have made the most of the particular features of organic semiconductors at the interface with biological systems.[1,2] The mixed ionic/electronic transport and the soft nature of these materials have proven an almost perfect match with both mechanical and conduction properties of most of biological systems, guaranteeing a straightforward and efficient signal transduction at the biotic−abiotic interface.[3] Therefore, and through the improvement of fabrication techniques and the design and synthesis of novel materials,[4,5] various devices have been developed with the aim of translating electronic signals into ionic ones and vice versa, such as soft actuators,[6] drug delivery devices,[7] recording and stimulation probes,[8,9] biosensors,[10,11] and organic electrochemical transistors (OECTs).[12,13]

In OECTs, particularly, an organic semiconductor film (channel) bridges source and drain electrodes, and its conductivity is regulated by the application of a gate voltage (V_G) through an electrolyte.[14] These devices operate as organic mixed ionic−electronic conductors since ion injection from the electrolyte into the organic film is required to maintain charge balance.[15] While this phenomenon grants them with record-high transconductance, it also limits their response time.[15,16] Since the appearance of OECTs, poly(3,4-

ethylenedioxythiophene) (PEDOT) and its water-stable colloidal complex with poly(styrenesulfonate) (PEDOT:PSS) have been extensively employed as a conducting channel material for the fabrication of said devices.[17] Nevertheless, as-prepared doped PEDOT yields devices that operate in depletion mode, requiring high operating currents as well as high V_G to keep the channel in the OFF state.[18] In addition, the application of these relatively elevated voltages can generate parasitic reactions with water and oxygen from the electrolyte, triggering the deterioration of the transistors.[4,19]

Another relevant challenge involves the integration of PEDOT with biological entities, which is usually hampered by the lack of functional groups in pristine films.[4] In addition, PEDOT:PSS displays some extra disadvantages due to the acidity/toxicity of PSS, which could prompt undesired reactions with materials adjoining the bioelectronic device active layer.[5] Moreover, since PSS is usually in excess in the conducting polymer−polyelectrolyte complex, the overall
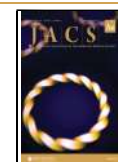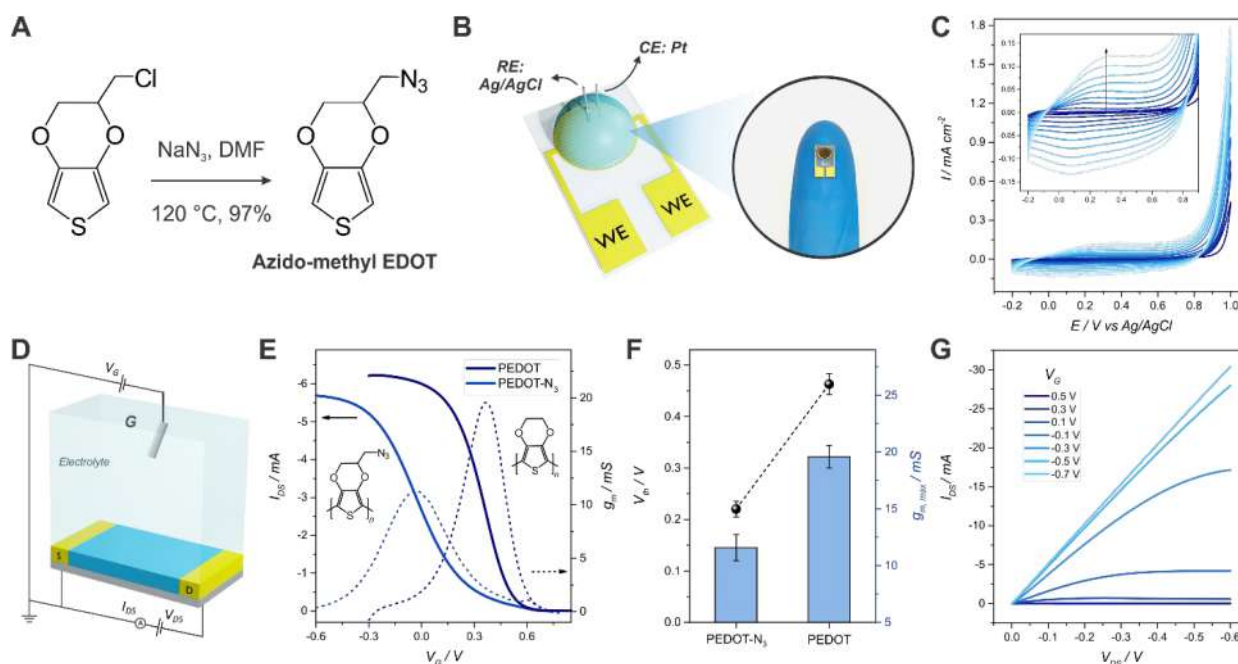
Figure 1. Scheme of the EDOT-N$_3$ monomer synthesis (A). Scheme of the electropolymerization setup employed for the fabrication of the transistors and photograph of an OECT after fabrication (B). Electropolymerization curves for a PEDOT-N$_3$-OECT (0.1 M HClO$_4$, 10 mM EDOT-N$_3$, 0.1 M KCl, 0.05 M SDS 0.05 M, 40 mV/s, 10 cycles) (C). Scheme of the setup employed for measurement of the electrical characteristics of the transistors (D). Transfer characteristics curves and transconductance for a PEDOT and a PEDOT-N$_3$ OECT obtained under the same electropolymerization conditions (V_{DS} = −0.1 V, 1× PBS) (E). Threshold voltage and maximum transconductance for both PEDOT and PEDOT-N$_3$-based OECTs (F). Output characteristics for PEDOT-N$_3$ OECTs (G).

negative charge of the obtained films restricts their interfacing with most proteins, nucleic acids, and cells, which are also negatively charged at physiological conditions.[20,21]

Therefore, during the last years, researchers have tried to tailor the surface of PEDOT and PEDOT:PSS films through different approaches, such as its blending with other polymers or biomolecules[13,22] or simply by postmodification of their surface.[20,23] Another effective strategy involves the synthesis (and subsequent polymerization) of EDOT derivatives containing recognition motifs which can be used for bioconjugation in a subsequent step. In this regard, several EDOT derivatives have been reported during the last two decades in the field of organic bioelectronics, such as carboxylic acid-functionalized-EDOT (EDOT-acid),[24,25] an EDOT derivative bearing an oxylamine moiety (EDOTOA),[26] hydroxymethyl-EDOT (EDOT-OH),[27] and an amino-modified EDOT (EDOT-NH$_2$),[28] among others.[29−31]

On the other hand, click chemistry comprises a set of reliable, efficient, and stereoselective reactions that allow for the construction of a wide range of molecules and architectures through the employment of harmless reaction conditions and accessible starting materials.[32,33] Among the various "click" reactions, the Huisgen 1,3-dipolar cycloaddition of azides and alkynes, generating 1,2,3-triazoles, is certainly the most known and employed one.[34] In this regard, the alkyne and azide moieties are relatively easy to synthesize and incorporate to different molecules, they are stable in a wide range of solvents (including water), and they are chemically inert toward most of the moieties present in biological entities, such as lipids, proteins, and nucleic acids (which makes them bio-orthogonal and biocompatible).[35] Therefore, these moieties are considered to be almost ideal building blocks for the construction of bioconjugation platforms through click chemistry.

Nevertheless, the application of this reaction was limited for more than 40 years by the necessity for high temperatures, long reaction times, and inferior regiospecificity (since both the 1,4- and 1,5-isomeric adducts were formed). It was not until the introduction of copper(I) catalysis and the discovery of the beneficial effects of water that this reaction was considered an essential tool in chemistry, and particularly for bioconjugation purposes.[34−36] Interestingly, the Cu(I) catalyst not only accelerates the azide−alkyne condensation kinetics by activating the slow-reacting alkyne moieties but also arranges the reacting groups, thus regioselectively yielding only the 1,4-disubstituted 1,2,3-triazole.[34,35] In addition, the copper-catalyzed reaction requires no protecting groups and proceeds with almost complete selectivity and conversion. These unique features have caused the Cu(I)-catalyzed azide alkyne cycloaddition (CuAAC) to be known as "The Click Reaction",[34] and have propelled its application within the fields of chemistry, biology, biochemistry, and biotechnology.[34,36−38]

In this context, researchers have applied azide−alkyne cycloadditions toward the development of various electrochemical and optical biosensing platforms.[39,40] Furthermore, azido-bearing PEDOT derivatives have been deposited on traditional electrodes, rendering surfaces with tunable features.[41−43] Regarding transistors, approaches based on azide−alkyne cycloadditions have been mainly used for the synthesis[44,45] and anchoring[46,47] of organic semiconductors for electronic applications, as well as for the surface modification of graphene and diketopyrrolopyrrole-based field-effect transistors.[48,49] However, and to the best of our knowledge, there has been no report toward the fabrication of a high-performance PEDOT-based organic transistor whose channel is prone to be modified by click chemistry.
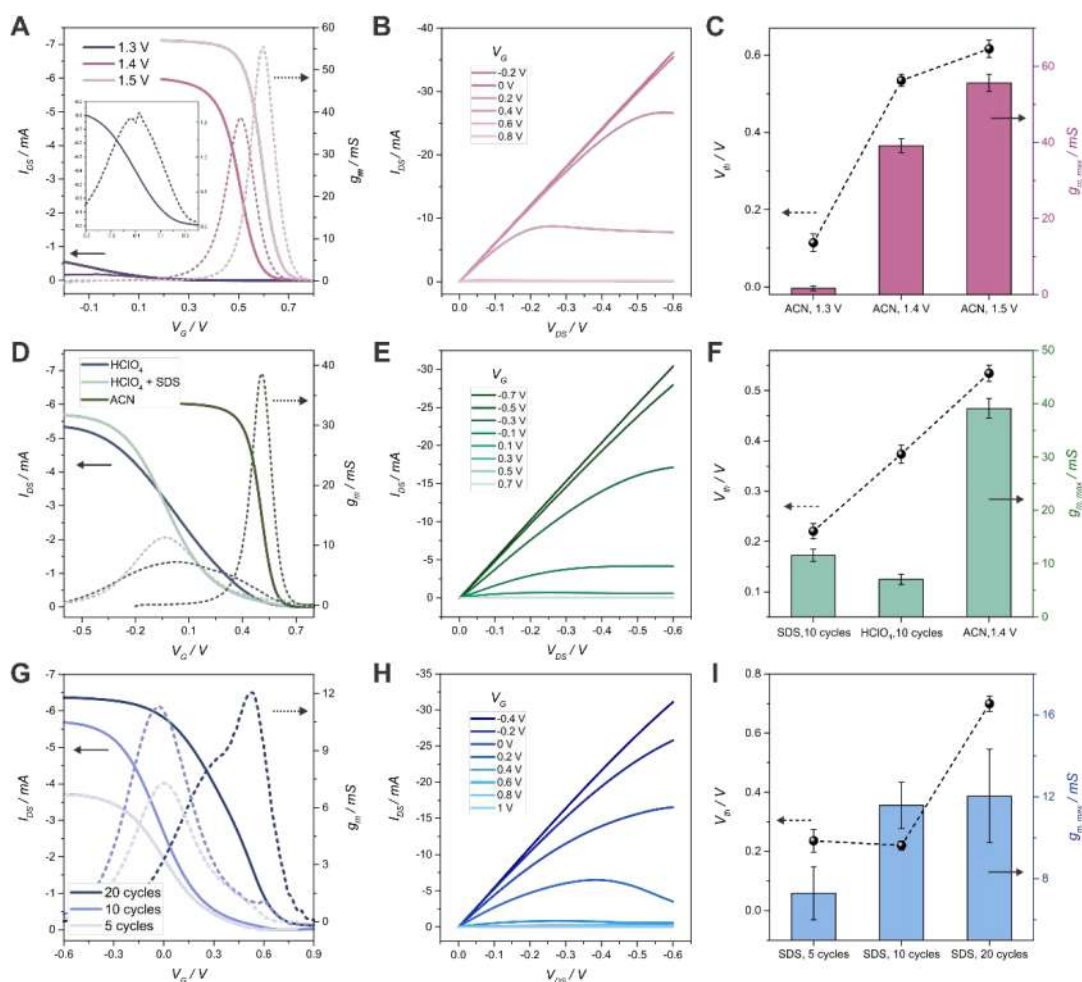
Figure 2. Transfer characteristics curves with the calculated transconductance, output characteristics curves, and threshold voltage and maximum transconductance values for PEDOT-N$_3$ OECTs obtained from (A)−(C) ACN 0.1 M TBAPF$_6$ electrolyte solutions for different anodic potential limit values ((B): output curves for 1.4 V), (D)−(F) ACN, HClO$_4$ and HClO$_4$+SDS (10 cycles) ((E): output curves for HClO$_4$+SDS) and (G)−(I) HClO$_4$+SDS solution varying the number of electropolymerization cycles from 5 to 20 ((H): output curves for 20 cycles) (EDOT-N$_3$ 10 mM and V_{DS} = −0.1 V, 1× PBS).

In this work, we present the first example of PEDOT-based "clickable" organic electrochemical transistors. We first report on the synthesis of an azide-derivatized EDOT monomer (azidomethyl-EDOT, EDOT-N$_3$) and its deposition on Au interdigitated electrodes to yield PEDOT-N$_3$-based OECTs. The obtained transistors show lower threshold voltages than PEDOT-based state-of-the-art devices, maximum transconductance voltages values close to 0 V, and high transconductance values, fundamental requirements for the development of efficient organic bioelectronic devices. Next, the clicking of ethynyl-bearing redox probes is performed and studied by means of cyclic voltammetry, as well as the clicking of biorecognition elements bearing biotin moieties, which is validated by means of Fiber-Optic Surface Plasmon Resonance (FO-SPR) spectroscopy. The biotin-clicked PEDOT-N$_3$ devices are used to anchor NeutrAvidin and streptavidin-conjugated horseradish peroxidase for the fabrication of relevant bioconstructs. Additionally, a strain-mediated click reaction is used for the anchoring of a thrombin specific dibenzocyclooctyne (DBCO)-modified HD22 aptamer, showing the application of the OECTs toward the development of cardiac biomarkers sensing devices. Very importantly, it is shown that the clicked OECTs maintain their electronic features after the different clicking procedures, demonstrating their stability and robustness.

RESULTS AND DISCUSSION

Fabrication and Optimization of Clickable OECTs

First, azido-bearing EDOT monomer (2-azidomethyl-3,4-ethylenedioxythiophene, EDOT-N$_3$) was synthesized from 2-chloromethyl-3,4-ethylenedioxythiophene, based on a previously reported protocol (Figure 1(A); Figure S1 and S2, Supporting Information (SI)).[50,51] Next, PEDOT-N$_3$-based OECTs were prepared by electrochemical polymerization of the EDOT-N$_3$ monomer on commercial interdigitated Au microelectrodes. To this end, both source and drain electrodes were shorted and employed as unique WE in a three-electrode-cell electrochemical setup (Figure 1(B)). An example of a typical electropolymerization curve is shown in Figure 1(C). The mechanism for the electrodeposition of conducting polymer films on interdigitated electrodes has been previously discussed by Musumeci et al.,[52] showing that low electric field strengths lead to the formation of thin films via progressive nucleation and 2D growth. Also, this technique has been recently exploited by Mawad and collaborators for the

straightforward fabrication of OECTs, showing its potential toward the development of bioelectronic devices.[53,54]

The electrical features of the transistors were evaluated by means of an electrolyte-gated setup, as shown in Figure 1(D). The obtained transfer (Figure 1(E)) and output (Figure 1(G)) characteristics curves show the typical features of depletion-mode transistors (similarly to other PEDOT-based OECTs[13,20]); i.e., when no gate voltage is applied, the OECTs exhibit the ON state. However, certain differences can be observed with respect to PEDOT-based OECTs (obtained by employing the same conditions), such as a lower threshold voltage (V_{th}) and transconductances ($g_{m,max}$) values (Figure 1(F) and Figure S12; other relevant parameters such as D-S resistivity are also compared in the SI). It is known that "pristine" PEDOT shows higher conductivity than the azide-derivatized polymer, which accounts for the higher transconductance values observed.[43] On the other hand, the lower threshold voltage and voltage of maximum transconductance ($V_{G,gm\ max}$) observed in PEDOT-N$_3$ OECTs are highly beneficial toward the development of organic bioelectronic platforms, yielding more energy-efficient devices as well as diminishing the alteration of bioentities that could be immobilized on the surface. The fabricated transistors also showed lower V_{th} than state-of-the-art OECTs using commercial PEDOT:PSS as channel material, which have shown a V_{th} of ~0.52 V.[55]

Next, the OECT fabrication protocol was optimized to obtain high performance transistors for the development of efficient organic bioelectronic devices. To this end, the effect of different factors such as electrolyte, potential window, and cycles number were evaluated for the electrodeposition of the polymer film on the interdigitated electrodes (IDEs). To benchmark the obtained devices, different parameters such as V_{th}, maximum transconductance ($g_{m,max}$), and $V_{G,gm\ max}$ were calculated (details are presented in the SI, Figure S8). Devices exhibiting low V_{th} and $V_{G,gm\ max}$ close to 0 V while preserving high $g_{m,max}$ are particularly desired; a reduction in the V_{th} diminishes the power consumption and simplifies the circuit design by allowing the use of only one power supply.[56,57] More importantly, the operation of the transistors at $V_G = 0$ V prevents the alteration of anchored bioentities, such as proteins, lipid bilayers, or cells, which could degrade at high applied voltages.[58] Similarly, the recognition processes are less affected by the application of (very) low electrical fields.[59]

Initially, the polymerization was performed in an organic solvent. Inhomogeneous films with high V_{th} and $V_{G,gm\ max}$ values were obtained, as shown in Figures 2(A)−(C) and S3. An increase of the anodic limit voltage only generated thicker polymer channel films, yielding (even) higher V_{th} and $V_{G,gm\ max}$. Moreover, the thickness and morphology of the film were difficult to control, probably due to the high electrolyte resistance in the organic media. When lower anodic voltages values were employed, very low $g_{m,max}$ values were obtained, and the stability of the devices was affected (Figure 2(C) and Figures S3−5).

Hence, by adapting a recently reported protocol,[60] polymer films from aqueous acidic solutions were prepared. Compared with those obtained in ACN, thinner and more homogeneous films were obtained, as observed in Figure S6. The obtained OECTs showed lower V_{th} and $V_{G,gm\ max}$, but the $g_{m,max}$ values of the devices were relatively low (Figure 2(D)−(F)). In addition, some irregularities were still found on the films,

probably due to the low solubility of the organic monomer in the acidic aqueous medium.

To solve this issue, the electrosynthesis of the polymer films on the IDEs was performed by employing an acidic microemulsion polymerization solution. SDS and KCl were added to the HClO$_4$ electrolyte to improve the solubility of the organic monomer. It has been previously reported that the electropolymerization of EDOTs from microemulsion solutions yields ultrasmooth PEDOT films on a variety of substrates showing very low RMS values.[61] Furthermore, it is known that SDS is able to dope PEDOT, increasing the conductivity of the polymer film and diminishing its oxidation potential.[4,62]

Next, optical microscope images of the obtained OECTs revealed homogeneous films (Figure S7). Moreover, compared to the OECTs obtained from the HClO$_4$ aqueous solutions and the same number of cycles, the transistors showed higher $g_{m,max}$ and lower V_{th} and $V_{G,gm\ max}$ values (Figure 2(E),(F)). These outcomes can be ascribed to the higher homogeneity of the obtained polymer films, leading to more efficient charge transport, as well as to the doping of PEDOT-N$_3$ by the anionic surfactant.

Subsequently, the effect of the number of electropolymerization cycles in the SDS solution was studied (Figure 2(G)−(I)). It can be observed that the transistors fabricated with 10 cycles showed relatively high $g_{m,max}$ while keeping low V_{th} and $V_{G,gm\ max}$. In comparison, the transistors obtained employing only 5 electropolymerization cycles showed lower transconductance and similar $V_{G,gm\ max}$ and V_{th}. On the other hand, an increase in the number of cycles to 20 yielded devices with barely improved transconductance while presenting too high $V_{G,gm\ max}$ and V_{th} values.

A comparison chart for all the polymerization conditions and further information regarding the electropolymerization in different solvents is shown in the SI (Figures S9 and S10). It is worth noting here that the use of interdigitated Au microelectrodes allowed for the preparation of devices with relatively high $g_{m,max}$ values compared to previously reported PEDOT-based OECTs.[63,64] In addition, the developed fabrication method showed high device-to-device reproducibility, since the RSD of resistance values for the finished OECTs was lower than 15% for 17 transistors (Figure S11). The measured resistance after a complete set of experiments showed changes lower than 5%, which accounts for the high stability of the devices. Finally, the previously mentioned results prompted the decision of using the transistors obtained by employing 10 electropolymerization cycles in an acidic microemulsion solution.

Characterization of Clickable OECTs

To verify the presence of the azide moieties after the electropolymerization protocol, ATR-FTIR measurements of the OECTs were performed. The spectrum of the PEDOT-N$_3$ film (obtained from the SDS-HClO$_4$ solution) showed the typical azide band at ca. 2100 cm^{-1} (Figure S16).[42] Furthermore, the spectrum showed the presence of PEDOT-N$_3$ bands as well as SDS ones, confirming the incorporation of the SDS anions into the polymer film during the electrosynthesis. Further description is presented in the SI.

To gain further insight into the PEDOT-N$_3$ fabricated OECTs, AFM measurements of the channel area of the devices were performed. The developed protocol yielded smooth PEDOT-N$_3$ films with a very low RMS value of 1 nm (Figure
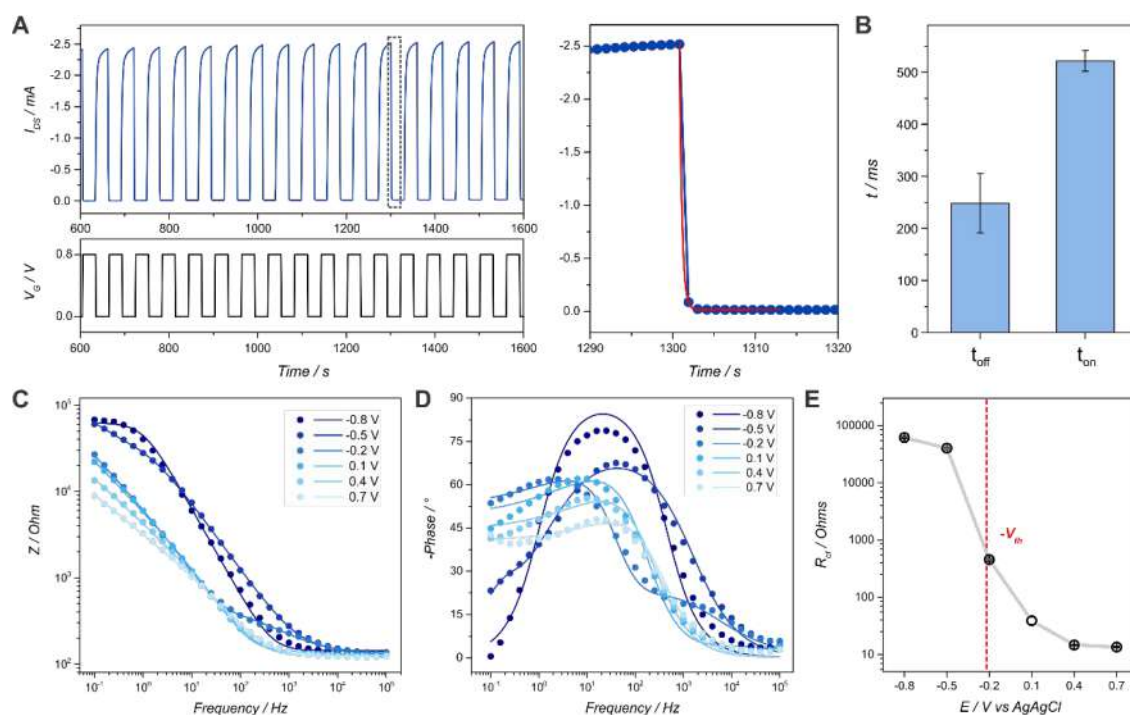
Figure 3. Transient characteristics of a PEDOT-N$_3$ OECT (left) and example of the fitting to obtain the t_{on} and t_{off} values (right) ($V_{DS} = -0.1$ V, 1× PBS) (C). t_{on} and t_{off} values obtained from the fitting of the curves ($n = 3$) (D). Potentiostatic EIS spectra for a PEDOT-N$_3$ electrode at different applied potentials: impedance (E) and phase (F) responses (1× PBS, 10 mV amplitude). Charge-transfer resistance obtained from the fitting of the EIS spectra and correlation with V_{th} (G).

S15). In addition, an average film thickness of 130 ± 11 nm was obtained from AFM measurements. Next, the electropolymerization technique endowed a reproducible and homogeneous film deposition with a very low surface roughness, which allowed high performance OECTs.

To further characterize the response of the clickable OECTs, the transient behavior of the devices was studied. This feature is particularly relevant when considering the interfacing of OECTs with biological entities, such as those required for neural and electrophysiological recording.[13,65] To this end, the repeated cycling of the OECTs between 0 V and the ON/OFF states was performed while recording the drain-source current (I_{DS}) at a constant drain source voltage (V_{DS}). The obtained source-drain current response was adjusted to an exponential decay to obtain t_{on} and t_{off} for each set of transistors, as previously described.[13,65,66] OFF-switching curves obtained for an OECT and an example of the fitting are shown in Figure 3(A), whereas ON-switching curves and their corresponding fitting are shown in the SI (Figure S13). Next, ON and OFF times of 522 ± 20 and 248 ± 57 ms, respectively, were found (Figure 3(B)). These values are in the same range as those previously reported for PEDOT−PAH[13] and PEDOT-S-based OECTs,[67] showing that the azide-derivatized PEDOT-based transistors can be employed for high-performance bioelectronics applications.[13]

Another pertinent attribute of OECTs is the I_{ON}/I_{OFF} ratio, particularly relevant in applications involving logic circuits and matrix active displays.[68] An I_{ON}/I_{OFF} ratio of 2352 ± 54 was obtained from the transfer characteristics curves. This value is substantially higher than those of recently reported PEDOT-based OECTs, such as PEDOT-phosphonate (618 ± 54),[69] PEDOT:PSS (541),[70] and PEDOT-S (650 ± 210) OECTs,[67]

which shows the potential application of the obtained devices in the above-mentioned fields.

Furthermore, to electrochemically characterize the polymer film obtained on the IDEs, potentiostatic electrochemical impedance spectroscopy (EIS) measurements were performed at different applied potentials (Figure 3(C),(D)). It is worth mentioning here that, while numerous circuits have been described for conducting polymer films, and particularly for PEDOT-based OECTs, the interpretation of the EIS response of conducting polymers is not simple.[71,72] Recently, the impedimetric behavior of PEDOT-based OECTs has been described as a combination of an electronic circuit, related to the charge transport in and to the channel material, and an ionic circuit, accounting for the ionic transport from the electrolyte to the polymer (more details are presented in the SI).[13,66]

From Figure 3(C) it can be observed that, as the applied potential increased, the low frequency impedance of the film decreases, in agreement with the oxidation of the polymer and the subsequent generation of charge carriers, rendering the film electrically conducting.[69] Moreover, in Figure 3(D) it is also observed that the phase shift at frequencies in the range of 10^1-10^3 Hz decreases in magnitude while increasing the applied potential, suggesting a change from a capacitive to resistive character, in accordance with previous reports.[69]

The fitting of the EIS response to a previously reported circuit is shown in the SI, together with the Nyquist plot of the spectra. These plots showed two regimes; at high frequencies, a semicircle with a radius proportional to the charge-transfer resistance was observed, while at low frequencies, a line with a slope at a 45° angle was exhibited, indicative of a mixed capacitive-impedance response which is dominated by the ionic exchange between the polymer film and the electrolyte.[69]
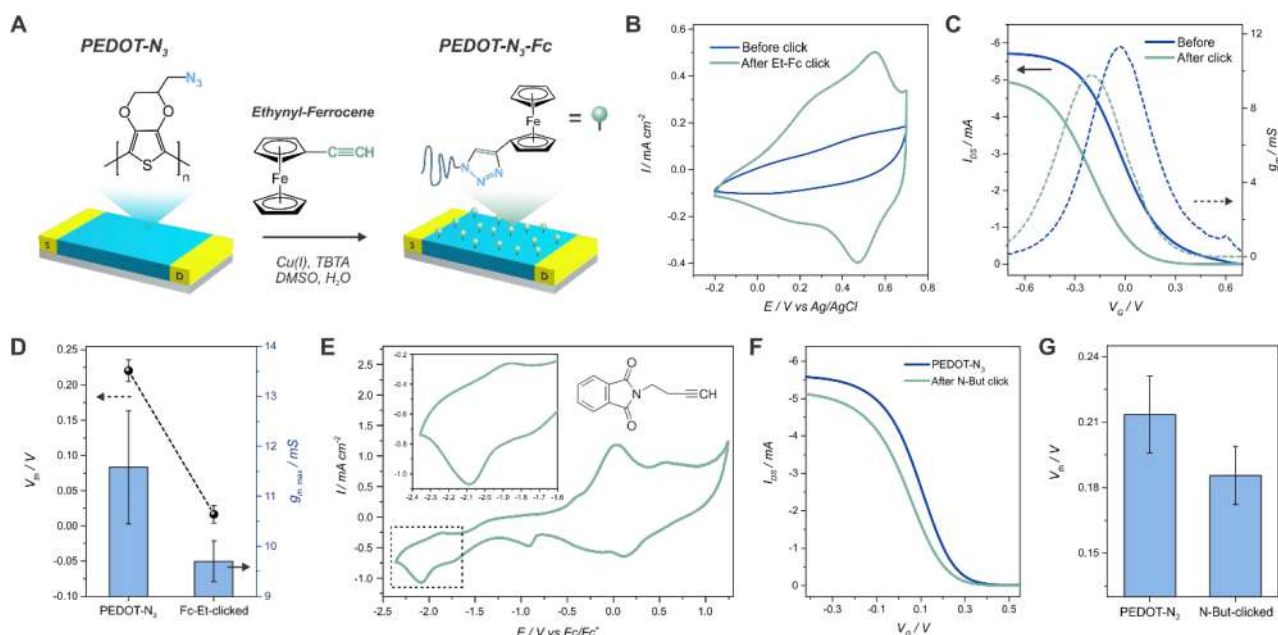
Figure 4. Scheme for the click functionalization of the PEDOT-N$_3$ OECTs with ethynyl-ferrocene (A). Cyclic voltammetry curves for a PEDOT-N$_3$ electrode before and after the click reaction with Et-Fc (50 mV/s, 1× PBS) (B). Transfer characteristics curves for a PEDOT-N$_3$ OECT before and after the click reaction with Et-Fc (V_{DS} = −0.1 V, 1× PBS) (C). Threshold voltage and maximum transconductance for a PEDOT-N$_3$ OECT before and after the click reaction with Et-Fc (n = 3) (D). Cyclic voltammetry curves for a PEDOT-N$_3$ electrode after the click reaction with N-But (50 mV/s, TBAF$_6$ 0.1 M, ACN) (E). Transfer characteristics curves for a PEDOT-N$_3$ OECT before and after the click reaction with N-But (V_{DS} = −0.1 V, 1× PBS) (F). Threshold voltage for a PEDOT-N$_3$ OECT before and after the click reaction with N-But (n = 3) (G).

The two regimes were more clearly identified at −0.2 V, while the radius of the semicircle became very small at higher potentials (Figure S14), suggesting a diminished charge transfer resistance as the film was oxidized. Next, when the obtained charge-transfer resistance is plotted against the potential applied (Figure 3(E)), a steep decrease of the value can be seen when the electrode is biased at more positive potentials than −0.22 V. This is in close agreement with the threshold voltage value determined for the PEDOT-N$_3$-based transistors in the previous section.

Furthermore, the capacitance as a function of the frequency was also calculated (Figure S14). It can be observed that the capacitance increased for more positive potentials, since the generation of polarons, and therefore, positive charges, induces the incorporation of counteranions, required to maintain the charge balance inside the film.[73] Next, the capacitance at 0.1 Hz and 0.7 V for the polymer film was extracted, and a volumetric capacitance of 226 ± 92 F cm^{-3} was obtained by considering the volume of the film. This value significantly surpasses the one informed for ethylene glycol-treated PEDOT:PSS OECTs (C^* = 39 ± 3 F cm^{-3}), a widely employed OECT material,[74] as well as that of recently reported high-performance PEDOT−PAH OECTs (74 ± 2 F cm^{-3}),[13] and is similar to the values obtained for other state-of-the-art OECTs, such as p(g2T-T) (C^* = 241 ± 94 F cm^{-3}).[18,75] Then, the high volumetric capacitance and transconductance values shown by PEDOT-N$_3$-based OECTs make this conducting polymer a promising alternative toward the development of efficient electronic devices.

Clicking of Redox Molecules

To corroborate the availability of the azide moieties of the PEDOT-N$_3$ conducting channel after the electropolymerization, the transistors were functionalized with an ethynyl-bearing redox probe, ethynyl-ferrocene (Et-Fc), via a DMSO/

H$_2$O-based copper(I)-catalyzed Huisgen 1,3-dipolar cyclo-addition ("click" reaction), as depicted in Figure 4(A).

Figure 4(B) shows the cyclic voltammetry curves of a PEDOT-N$_3$ electrode (both S and D electrodes of the OECT were connected as a WE, as performed for the electro-polymerization) before and after the click reaction. The redox peaks of the ferrocene couple can be observed after the click reaction at 0.51 V (0.55 and 0.47 V for the oxidation and the reduction process, respectively), confirming the effective clicking of the redox probe (control experiments performed employing PEDOT without azide moieties are shown in the SI, Figure S17). Next, from these results, an estimated density of functionalized azide moieties can be calculated by employing the charge of the redox peaks, according to Γ = Q/nFA, where Q is the passed charge, n is the number of electrons transferred (n = 1), F is the Faraday constant, and A is the electroactive surface area of the electrode (9.62 mm^2). The averaged charge for the oxidation and reduction of ferrocene correlates to a density of (3.0 ± 0.6) × 10^{-10} mol cm^{-2}.

When considering the transfer characteristics of the transistors (Figure 4(C)) it can be observed that, upon Et-Fc clicking, the $V_{G,gm\ max}$ and the V_{th} are diminished by ∼170 and ∼200 mV, respectively. Moreover, the ON I_{DS} diminishes by 14%, and the transconductance does so by 16%. These outcomes could have two origins; first, the swelling produced by DMSO[76] can create a more porous structure, resulting in additional ion conduction channels, which is known to shift the V_{TH} of the transistors to more negative potentials.[13,64] The increase in the capacitive current observed in the CV measurements upon clicking (as well as the similar V_{TH} shift observed when an acetylene-PEG$_4$-biotin was clicked, see the next section) supports this hypothesis. On the other hand, the incorporation of the ferrocene molecule could also be a reason. In this regard, it has been recently stated that the presence of a
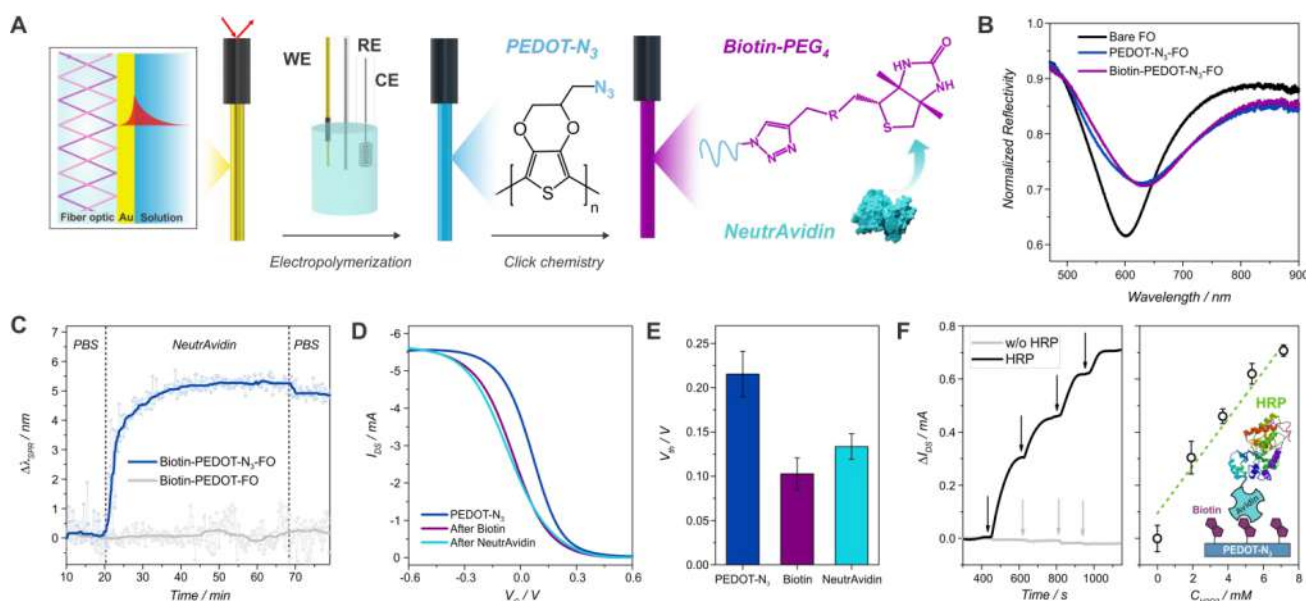
Figure 5. Scheme of the FO-SPR setup and the steps involved in the click functionalization of the fibers (A). FO SPR spectra of a bare fiber, after PEDOT-N$_3$ electropolymerization and click of the acetylene-PEG$_4$-biotin (B). Kinetic experiment of the NeutrAvidin binding for the biotin-PEDOT-N$_3$-FO (raw and smoothed data) (C). Transfer characteristics curves of a PEDOT-N$_3$ OECT before, after the click reaction with acetylene-PEG$_4$-biotin and after NeutrAvidin recognition (V_{DS} = −0.1 V, 1× PBS) (D), and threshold voltage obtained from the transfer curves (n = 3) (E). Recorded change in I_{DS} of an HRP-streptavidin-biotin-PEDOT-N$_3$-OECT (and control experiment without HRP) (left) and its dependence with the concentration of H$_2$O$_2$ (right) (V_{DS} = −0.1 V, V_G = 0 V, 1× PBS) (F).

redox couple on the gate electrode can be used to easily modulate the threshold voltage of OECTs.[58,77] However, in our case, the gate electrode employed for the measurements was a Ag/AgCl reference electrode and no electroactive species were bound to it.

Finally, the output characteristics of the devices after the click reaction (Figure S18) show that the transistors keep their performance after the click functionalization. Therefore, the transistors are fully functional after the clicking process in the organic solvent and the multiple cycling procedures in the PBS solution, indicating their high stability and robustness, as well as the possibility of modifying their surface with a desired molecule.

Similarly, the "electro"clicking of the alkyne bearing redox couple N-(3-butynyl)phthalimide (N-But) was also performed on the PEDOT-N$_3$ OECTs, by adjusting a previously reported protocol.[78] The cyclic voltammetry curves after the clicking reaction are shown in Figure 4(E) (Figure S20 shows the curves before and after the click process). In agreement with previously reported results,[42,79] the peaks of the redox couple at about −2 V (vs Fc/Fc$^+$) can be observed after the clicking procedure, corroborating the effectiveness of the reaction.

Moreover, the transfer characteristics of the devices showed a slight reduction in the V_{TH} of ∼30 mV (Figure 4(F)−(G)). This small shift suggests that PEDOT-N$_3$ does not experience a swelling as the one observed when performing the clicking in DMSO, and therefore, the clicking reaction would probably be more confined to the surface of the polymer.[76] Therefore, one might be able to spatially control the reach of the click reaction by carefully choosing the clicking protocol. Finally, the output characteristics of the N-But-clicked OECTs are shown in Figure S21, confirming that the devices still perform normally after the clicking and the CV measurements.

The above-mentioned results confirm that it is possible to click redox molecules to the OECTs without altering their proper operation. The high stability of the OECTs in different electrolytes and solvents allows for the employment of different functionalization procedures, providing the possibility of clicking different molecules without solubility issues and controlling their spatial distribution.

Clicking of Biorecognition Elements

Next, to evaluate the anchoring of biorecognition entities to the organic transistors toward the development of organic bioelectronic platforms, the click reaction of an acetylene-PEG$_4$-biotin on the PEDOT-N$_3$ transistors was evaluated by means of a fiber-optic surface plasmon resonance (FO-SPR) setup, and the further recognition of NeutrAvidin was assessed. The biotin−avidin complex has been widely employed toward the development of biosensing devices as well as in other biotechnology applications due to the its high affinity constant, leading to reliable and stable biomolecular constructs.[80]

Next, PEDOT-N$_3$ films were electropolymerized on a Au-coated optical fibers (FO) by employing the same conditions as the ones used for the fabrication of the OECTs, using the gold-coated FO as WE (Figure 5(A) and SI). A typical electropolymerization curve for the deposition of PEDOT-N$_3$ on the FO is shown in Figure S22, exhibiting analogous features as those observed on the IDEs and therefore validating the FO-SPR experiments. The deposition of the polymer film leads to a shift of the resonance wavelength (minimum of the reflected spectrum) to higher wavelengths of 33 ± 6 nm (three measurements performed) and a decrease in coupling intensity, as shown in Figure 5(B). These changes are attributed to the growth of a PEDOT-N$_3$ film with a thickness of 68 ± 5 nm (derived from the CV measurements). The observed spectral shift was evaluated using simulations based on the Fresnel reflectivity model (see the SI, Figure S26), and the obtained optical properties of the film are in good agreement with previously reported results for PEDOT films.[81]
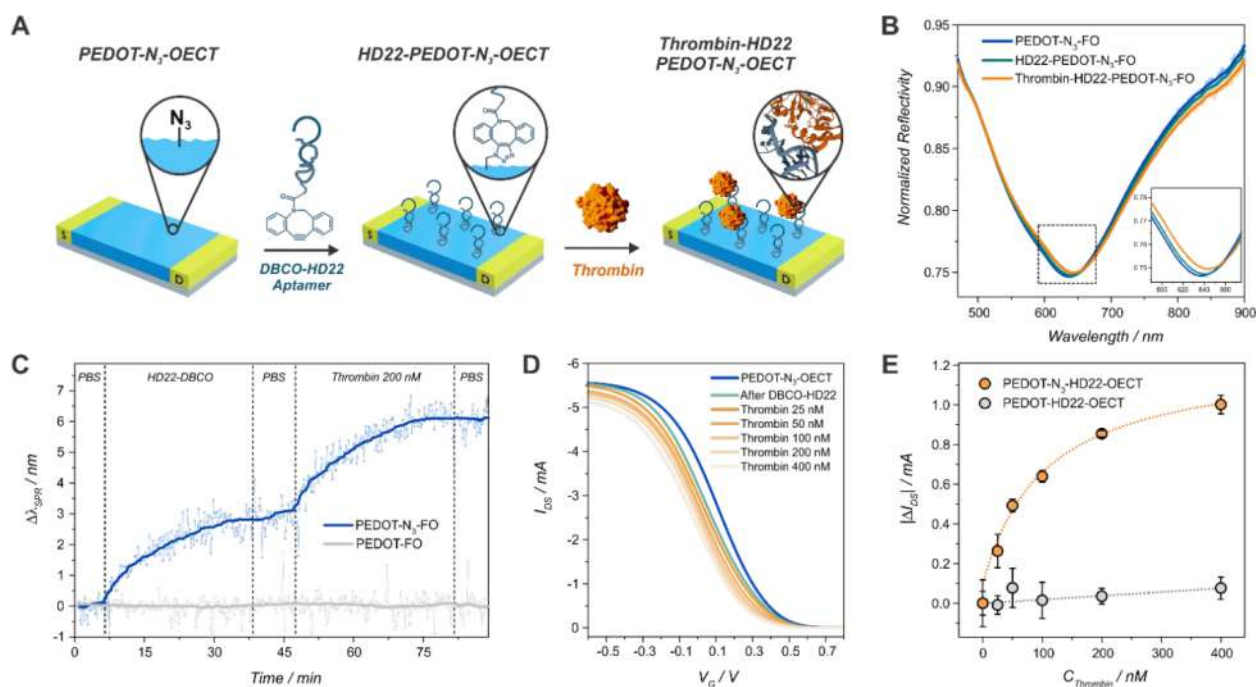
Figure 6. Scheme of the clicking of the DBCO-HD22 aptamer on the OECTs and the further thrombin recognition (A). Normalized reflectivity spectra (B) and kinetic experiment (C) of a FO modified with a film of PEDOT-N$_3$ after DBCO-HD22 clicking and thrombin recognition (C). Transfer characteristics curves of a PEDOT-N$_3$-OECT before and after DBCO-HD22 functionalization and further thrombin recognition (V_{DS} = −0.1 V, 1× PBS) (D). Change in I$_{DS}$ obtained from the transfer characteristics for a PEDOT-N$_3$-HD22 OECT and control experiment with a PEDOT OECT (n = 3) (E).

Next, to incorporate biorecognition moieties to the surface, the click of an alkyne-PEG$_4$-biotin was performed. Upon biotin clicking, the resonance wavelength shifts to higher wavelengths by 5.6 ± 0.3 nm (average for two measurements), indicating the successful clicking of the alkyne-bearing biotin-PEG$_4$ on the PEDOT-N$_3$ modified fiber (Figure 5(B) and SI). This shift can be correlated to a surface mass density of 339 ± 26 ng/cm^2 (see the SI).

Subsequently, the recognition of NeutrAvidin was evaluated in a kinetic experiment by tracking the resonance wavelength over time (Figure 5(C)). Upon NeutrAvidin recognition, a shift in the resonance wavelength to higher values is observed, indicating that the avidin-bearing molecules are assembled on the biotin-modified polymer. The process achieves a plateau after 20 min, in accordance with previous reports,[80,82] and a shift of 5.6 ± 1.0 nm (n = 2) is observed. This shift can be correlated to a surface mass density of 328 ± 56 ng/cm^2 (see the SI). Control experiments were performed by carrying out the same steps for the FO functionalization on a PEDOT film (Figures S27 and S28), showing the specificity of the click reaction and the subsequent NeutrAvidin binding (Figure 5(C)).

Later, the same functionalization process was performed on the PEDOT-N$_3$ OECTs (Figure 5(D)). Upon the clicking of the acetylene-biotin, a shift of the V_{TH} of ~110 mV toward more negative potentials is registered, in line with the results observed for the clicking of Et-Fc. The further recognition of the NeutrAvidin causes a positive shift of the V_{TH} by 30 mV, ascribed to the binding of the negatively charged protein (isoelectric point of 6.3),[83] which causes the induction of positive charges in the organic semiconducting channel. The output characteristics curves after the whole modification process (Figure S27) account for the excellent stability of the

transistors since they preserve their features as amplification devices.

Next, as a proof of concept for the use of the clickable OECTs for the development of enzymatic biosensing devices, the biotin−avidin recognition was employed to assemble streptavidin-conjugated horseradish peroxidase (HRP) to the biotin-modified OECTs. Next, the devices were biased at the $V_{gm,max}$ (0 V, Figure S30) and H$_2$O$_2$ was continuously added to the electrolyte while registering the I_{DS}. Upon the addition of H$_2$O$_2$ in the millimolar range, the I_{DS} increases, showing that the enzyme preserves its functionality upon recognition from the biotin-clicked surface and the devices properly function as enzymatic biosensors for the sensing of H$_2$O$_2$ (Figure 5(F)). The transduction mechanism of the HRP enzymatic biosensors has been described as a direct electron transfer from the enzyme to the conducting polymer film.[84,85] Next, the recorded signal is greatly enhanced by the high $g_{m,max}$ of the device, making the changes easily observable. In addition, the $V_{G,gm\ max}$ presenting values close to 0 V allows the sensing of H$_2$O$_2$ without requiring the use of high gate voltages which can cause parasitic reactions or noise in the signal.[13] In this sense, while a thicker film could increase the $g_{m,max}$ of the OECTs it would also increase the $V_{gm,max}$ and might even hinder the electronic transport throughout the PEDOT-N$_3$ film, affecting the response of the biosensors.

Finally, the above-mentioned results show that the PEDOT-N$_3$ OECTs can function as stable and tunable platforms toward the development of organic bioelectronic devices through click chemistry, allowing the functional incorporation of biorecognition elements and enzymes without altering their proper functioning.

Clicking of Aptamers and Thrombin Recognition

As a proof of concept for the fabrication of aptamer-based biosensing devices based on PEDOT-N_3 OECTs (Figure 6(A)), the copper-free strain-promoted clicking of a thrombin specific DBCO-derivatized HD22 aptamer (known to interact with the exosite II of thrombin[86]) was performed. Thrombin is a kind of serine protease which plays an essential role in clot promotion and inhibition, and its imbalance can lead to bleeding or thrombosis.[87] Therefore, its determination in blood is of crucial relevance for the monitoring of patients which are exposed to invasive procedures such as dialysis or various surgeries.[88]

First, the click reaction of the DBCO-aptamer and its affinity for thrombin were investigated by means of the FO-SPR setup. To this end, a film of PEDOT-N_3 was electropolymerized on the fiber as described above, and the clicking process was started by dipping the fiber in a 1 μM DBCO-HD22 PBS solution. Later, and after a washing step with PBS, the fiber was immersed in a 200 nM solution of thrombin to evaluate the recognition of thrombin by the aptamer-modified surface. The whole process was followed by measuring the reflected spectra (Figure 6(B)) and monitoring the resonance wavelength over time, as shown in Figure 6(C). It is observed that the aptamer binds to the polymer-modified fiber, yielding a shift of the resonance wavelength of 3.1 ± 0.4 nm, corresponding to a surface mass density of 154 ± 27 ng/cm^2 (see the SI). This result indicates a significant increase in surface mass density of the HD22 aptamer on the PEDOT-N_3 film compared to previously reported surface architectures based on PEG-thiol self-assembled monolayers or polymer brushes.[89,90] This result can be attributed tentatively to the porous structure of the polymer film and the associated high surface area with a high density of clickable groups. After the washing of the surface with PBS, the immersion of the aptamer-modified fiber in a 200 nM thrombin solution in PBS results in a resonance wavelength shift of 3.0 ± 0.3 nm due to the recognition and binding of the cardiac biomarker by the aptamer-modified fiber tip. This shift can be correlated to a thrombin surface mass density of 193 ± 25 ng/cm^2 (SI). Furthermore, the experiment was contrasted to a fiber modified with PEDOT without azide moieties, and no aptamer nor thrombin unspecific adsorption was detected (Figure 6(C)).

Next, the thrombin sensing assay was performed also by the clickable transistors. To this end, the PEDOT-N_3 OECTs were functionalized with the DBCO aptamer and incubated in the respective thrombin solutions, and the transfer characteristic curves were measured. From Figure 6(D), the clicking of the aptamer generates a negative shift in the V_{TH} of 33 mV. Next, it is observed that all of the clicking of the different molecules (N-but, Et-Fc, acetylene-biotin-PEG$_4$ and DBCO-HD22) to the PEDOT-N_3 OECTs cause a shift of the V_{TH} to more negative potentials. This result can be ascribed to the conversion of the azide moieties of PEDOT-N_3 into triazole units, which can originate new ionic transport paths upon the alteration of the packing structure of the polymer.[49]

On the other hand, the thrombin recognition also results in a negative shift of the V_{TH} (Figure 6(E)), which is translated in a decrease of the registered I_{DS}. This effect has been previously reported in organic field effect transistors, and it is ascribed to the induction of negative charges in the semiconductor by the positively charged thrombin molecules.[91]

Later, the I_{DS} values for $V_G = 0$ V were computed and fitted to a Hill ($n = 1$) adsorption model, yielding a K_D for the DBCO-HD22-functionalized OECTs toward thrombin of 103 ± 44 nM (R^2=0.98), in good agreement with previously reported results.[86,92] In addition, a LOD of 31 nM was obtained. A comparison with others OECTs-based biosensing devices is shown in Table S3. The output characteristics of the devices measured after the recognition of 400 nM thrombin show the proper stability of the devices (Figure S32).

As a control experiment, PEDOT-based OECTs were fabricated by employing the same preparation process (see the SI, Figure S31), and the same protocol for the functionalization of the PEDOT-N_3 transistors was followed. The change in the current obtained from the transfer characteristics of the devices is shown in Figure 6(E). Almost no change is detected in the recorded I_{DS} of the PEDOT transistor upon exposition to different thrombin solutions, confirming the effective functionalization and specificity of the PEDOT-N_3-based biosensing devices.

CONCLUSIONS

We have shown the development of PEDOT-N_3-based organic electrochemical transistors. The fabrication of PEDOT-N_3 OECTs through electropolymerization of the EDOT-N_3 monomer on Au IDEs was performed, and the obtained devices showed lower V_{th} and $V_{g,gm\ max}$ values than state-of-the-art PEDOT-based transistors. Next, the azide moieties were employed to click acetylene-modified redox probes, such as N-(3-butynyl)phthalimide and ethynylferrocene. More importantly, the clicking of acetylene-PEG$_4$-biotin on the transistors allowed for the fabrication of stable bioconstructs through avidin−biotin recognition, showing the potential of these devices for interfacing bioentities. In addition, a DBCO-modified thrombin-specific HD22 aptamer was clicked via a strain-promoted [3 + 2] azide−alkyne cycloaddition, allowing the further recognition of thrombin by the OECTs, yielding PEDOT-N_3-OECT-based biosensing devices.

We believe that this work can pave the way toward the straightforward and controlled design of organic bioelectronic devices through the use of the well-known toolbox of click chemistry.

MATERIALS AND METHODS

Synthesis of EDOT-N_3

2-Azidomethyl-2,3-dihydrothieno[3,4-*b*][1,4]dioxine (EDOT-N$_3$). Under an inert atmosphere, 342 mg (5.24 mmol) of sodium azide was added to a magnetically stirred solution of 500 mg (2.62 mmol) 2-chloromethyl-2,3-dihydrothieno[3,4-*b*][1,4]dioxine in 25 mL of dry DMF. The reaction mixture was heated to 120 °C for 3 h. After cooling, 50 mL of water was added to the reaction mixture, and the product was extracted three times with 50 mL of diethyl ether each. The organic phases were combined, washed with 50 mL of water and 50 mL of brine, and dried over MgSO$_4$. Subsequently, diethyl ether was evaporated, and the crude product was purified over silica gel using petrol ether/ethyl acetate 95:5 as eluent, yielding 407 mg (78%) of EDOT-N_3 as a colorless oil.

Electrochemical Measurements

EIS and CV experiments were performed with an Autolab potentiostat with both source and drain electrodes of the IDEs connected as WE. For the aqueous measurements, an Ag/AgCl reference electrode and a Pt wire as CE were employed. The electrolyte solution used was 1× PBS. Potentiostatic EIS measurements were performed in the frequency range from 0.1 to 10^5 Hz, employing voltages ranging from −0.8 to 0.7 V.

Transistor Measurements

Transistor measurements were performed by means of a Keithley 4200-SCS probe station. For the transfer and the transient characteristics, the V_{DS} was kept fixed at −0.1 V. For the output characteristics, different gate voltages were employed in order to cover both ON and OFF states of the transistors, and they are reported in every plot (for instance, from −0.6 to 0.8 V, every 0.2 V). The V_{DS} was swept from 0 to 0.6 V. All of the measurements were performed in 1× PBS.

FO-SPR Measurements

FO-SPR measurements were performed by optically connecting the tips to a Y-optical splitter via a commercially available bare fiber terminator (Thorlabs, Inc.). Polychromatic light from a halogen light source (12 V, HL-2000-LL, Ocean Insight) was coupled into the input arm of the Y-optical splitter, guided to the fiber tip, back-reflected at the gold-coated cross section of the tip, and guided through the output arm of the splitter to a spectrometer (HR4000, Ocean Insight). The reflected light spectrum was normalized by the spectrum of the fiber in air before surface modification and processed by a dedicated LabView software. For electropolymerization, the upper gold-coated part of the fiber was connected using a conductive copper tape (Reichelt Elektronik GmbH & Co. KG). At the transition from SPR-zone to upper gold coated part of the fiber, a layer of conductive silver paint (RS Components Ltd.) was applied and subsequently coated with a layer of liquid heat shrink tubing (Performix Liquid Tape, Plastidip, Plasti Dip Europe GmbH) to ensure electrical connection across the transition as well as a constant electrode area.

Click Chemistry and Bioconjugation Protocols

The DMSO/H_2O-based procedure for the clicking of Et-Fc and Acetyele-PEG_4-biotin was adapted from a previously reported protocol.[93] Next, 4.5 μL of a 1:2 $CuSO_4\cdot5H_2O$ 0.05 M and TBTA 0.05 M in 3:1 DMSO-*tert*-butanol were mixed with 3 μL of 1 mM alkyne in DMSO, 4.11 μL of H_2O Milli-Q, 13.1 μL of DMSO, and 2.25 μL of NaAsc 0.1 M in Milli-Q and subsequently deposited on the modified area of the PEDOT-N_3−-OECTs. Finally, the electrodes were thoroughly washed with DMSO, KCl 3 M, and Milli-Q water and dried. To perform the clicking procedure on the PEDOT-N_3-modified FO, the final volume of the mixture was adjusted to 200 μL.

The "electro"click protocol was adapted from a previous report.[78] Chronoamperometry was performed at a constant potential of −0.75 V vs Ag/Ag^+ for 10 min in a DMF electrolyte solution containing 10 mM N-But and 2 mM $CuSO_4\cdot5H_2O$. Next, the electrodes were thoroughly rinsed with DMF and ACN and dried with N_2.

The recognition of neutravidin by the biotin-modified OECTs was performed by dipping the previously modified biotin-PEDOT-N_3 OECTs in a 0.3 mg/mL NeutrAvidin solution in 1× PBS for 45 min. Next, the electrodes were rinsed with 1× PBS and dried with N_2. To perform the recognition procedure on the PEDOT-N_3-modified FO, the final volume of the solution was adjusted to 200 μL.

The assembly of HRP-Streptavidin was performed by dipping the previously modified biotin-PEDOT-N_3-OECTs in the as-supplied commercial HRP-Streptavidin solution for 60 min. Next, the electrodes were rinsed with 1× PBS and dried with N_2.

Based on the FO-SPR results, the clicking of the DBCO-modified thrombin HD22 aptamer was performed in aqueous solution by immersing the azide-bearing electrodes in a 1 μM DBCO-HD22 1× PBS solution by 60 min. The electrodes were subsequently rinsed with 1× PBS and dried with N_2. Regarding the recognition of thrombin by the HD22-transistors, the aptamer-modified OECTs were incubated in the respective thrombin solution for 30 min, rinsed with 1× PBS, and dried with N_2.

More details of the materials and methods can be found in the Supporting Information.

■ ASSOCIATED CONTENT

Data Availability Statement

The data that support the findings of this study are openly available in Zenodo (DOI: 10.5281/zenodo.6794195).

Ⓢ Supporting Information

The Supporting Information is available free of charge at https://pubs.acs.org/doi/10.1021/jacsau.2c00515.

> Materials and Methods section, optimization, and comparison of the OECT obtention protocols, control experiments for the clicking of redox probes and aptamers, FO-SPR, ATR, FTIR, EIS, CV, and further measurements (PDF)

■ AUTHOR INFORMATION

Corresponding Authors

Gonzalo E. Fenoy − *AIT Austrian Institute of Technology GmbH, 3430 Tulln an der Donau, Austria; Instituto de Investigaciones Fisicoquímicas Teóricas y Aplicadas, Departamento de Química, Facultad de Ciencias Exactas, Universidad Nacional de La Plata − CONICET, 1900 La Plata, Argentina;* ⓞ orcid.org/0000-0003-4336-4843; Email: Gonzalo.Fenoy@ait.ac.at

Omar Azzaroni − *Instituto de Investigaciones Fisicoquímicas Teóricas y Aplicadas, Departamento de Química, Facultad de Ciencias Exactas, Universidad Nacional de La Plata − CONICET, 1900 La Plata, Argentina;* ⓞ orcid.org/0000-0002-5098-0612; Email: omarazzaroni@quimica.unlp.edu.ar

Peter Bäuerle − *Institute for Organic Chemistry II and Advanced Materials, University of Ulm, 89081 Ulm, Germany;* ⓞ orcid.org/0000-0003-2017-4414; Email: Peter.Baeuerle@uni-ulm.de

Wolfgang Knoll − *AIT Austrian Institute of Technology GmbH, 3430 Tulln an der Donau, Austria; Department of Scientific Coordination and Management, Danube Private University, 3500 Krems, Austria;* ⓞ orcid.org/0000-0003-1543-4090; Email: Wolfgang.Knoll@ait.ac.at

Authors

Roger Hasler − *AIT Austrian Institute of Technology GmbH, 3430 Tulln an der Donau, Austria;* ⓞ orcid.org/0000-0002-0883-3053

Felice Quartinello − *Department of Agrobiotechnology, IFA-Tulln, Institute of Environmental Biotechnology, 3430 Tulln an der Donau, Austria*

Waldemar A. Marmisollé − *Instituto de Investigaciones Fisicoquímicas Teóricas y Aplicadas, Departamento de Química, Facultad de Ciencias Exactas, Universidad Nacional de La Plata − CONICET, 1900 La Plata, Argentina;* ⓞ orcid.org/0000-0003-0031-5371

Christoph Lorenz − *Institute for Organic Chemistry II and Advanced Materials, University of Ulm, 89081 Ulm, Germany*

Complete contact information is available at:
https://pubs.acs.org/10.1021/jacsau.2c00515

Author Contributions

The manuscript was written through contributions of all authors. All authors have given approval to the final version of the manuscript. CRediT: **Gonzalo Eduardo Fenoy** conceptu-

■ REFERENCES

(1) Malliaras, G.; McCulloch, I. Introduction: Organic Bioelectronics. *Chem. Rev.* **2022**, *122* (4), 4323−4324.

(2) Berggren, M.; Richter-Dahlfors, A. Organic Bioelectronics. *Adv. Mater.* **2007**, *19* (20), 3201−3213.

(3) Mariano, A.; Lubrano, C.; Bruno, U.; Ausilio, C.; Dinger, N. B.; Santoro, F. Advances in Cell-Conductive Polymer Biointerfaces and Role of the Plasma Membrane. *Chem. Rev.* **2022**, *122* (4), 4552−4580.

(4) Fenoy, G. E.; Azzaroni, O.; Knoll, W.; Marmisollé, W. A. Functionalization Strategies of PEDOT and PEDOT:PSS Films for Organic Bioelectronics Applications. *Chemosensors* **2021**, *9* (8), 212.

(5) Kukhta, N. A.; Marks, A.; Luscombe, C. K. Molecular Design Strategies toward Improvement of Charge Injection and Ionic Conduction in Organic Mixed Ionic-Electronic Conductors for Organic Electrochemical Transistors. *Chem. Rev.* **2022**, *122* (4), 4325−4355.

(6) Smela, E. Conjugated Polymer Actuators for Biomedical Applications. *Adv. Mater.* **2003**, *15* (6), 481−494.

(7) Uguz, I.; Proctor, C. M.; Curto, V. F.; Pappa, A. M.; Donahue, M. J.; Ferro, M.; Owens, R. M.; Khodagholy, D.; Inal, S.; Malliaras, G. G. A Microfluidic Ion Pump for In Vivo Drug Delivery. *Adv. Mater.* **2017**, *29* (27), 1701217.

(8) Bianchi, M.; De Salvo, A.; Asplund, M.; Carli, S.; Di Lauro, M.; Schulze-Bonhage, A.; Stieglitz, T.; Fadiga, L.; Biscarini, F. Poly(3,4-ethylenedioxythiophene)-Based Neural Interfaces for Recording and Stimulation: Fundamental Aspects and In Vivo Applications. *Adv. Sci.* **2022**, *9*, 2104701.

(9) Berggren, M.; Głowacki, E. D.; Simon, D. T.; Stavrinidou, E.; Tybrandt, K. In Vivo Organic Bioelectronics for Neuromodulation. *Chem. Rev.* **2022**, *122* (4), 4826−4846.

(10) Marks, A.; Griggs, S.; Gasparini, N.; Moser, M. Organic Electrochemical Transistors: An Emerging Technology for Biosensing. *Adv. Mater. Interfaces* **2022**, *9* (6), 2102039.

(11) Koklu, A.; Ohayon, D.; Wustoni, S.; Druet, V.; Saleh, A.; Inal, S. Organic Bioelectronic Devices for Metabolite Sensing. *Chem. Rev.* **2022**, *122* (4), 4581−4635.

(12) Torricelli, F.; Adrahtas, D. Z.; Bao, Z.; Berggren, M.; Biscarini, F.; Bonfiglio, A.; Bortolotti, C. A.; Frisbie, C. D.; Macchia, E.; Malliaras, G. G.; McCulloch, I.; Moser, M.; Nguyen, T.-Q.; Owens, R. M.; Salleo, A.; Spanu, A.; Torsi, L. Electrolyte-Gated Transistors for Enhanced Performance Bioelectronics. *Nat. Rev. Methods Prim.* **2021**, *1* (1), 66.

(13) Fenoy, G. E.; Bilderling, C.; Knoll, W.; Azzaroni, O.; Marmisollé, W. A. PEDOT:Tosylate-Polyamine-Based Organic Electrochemical Transistors for High-Performance Bioelectronics. *Adv. Electron. Mater.* **2021**, *7* (6), 2100059.

(14) Rivnay, J.; Inal, S.; Salleo, A.; Owens, R. M.; Berggren, M.; Malliaras, G. G. Organic Electrochemical Transistors. *Nat. Rev. Mater.* **2018**, *3* (2), 17086.

(15) Berggren, M.; Crispin, X.; Fabiano, S.; Jonsson, M. P.; Simon, D. T.; Stavrinidou, E.; Tybrandt, K.; Zozoulenko, I. Ion Electron−Coupled Functionality in Materials and Devices Based on Conjugated Polymers. *Adv. Mater.* **2019**, *31*, 1970160.

(16) Khodagholy, D.; Rivnay, J.; Sessolo, M.; Gurfinkel, M.; Leleux, P.; Jimison, L. H.; Stavrinidou, E.; Herve, T.; Sanaur, S.; Owens, R. M.; Malliaras, G. G. High Transconductance Organic Electrochemical Transistors. *Nat. Commun.* **2013**, *4*, 1−6.

(17) Zeglio, E.; Inganäs, O. Active Materials for Organic Electrochemical Transistors. *Adv. Mater.* **2018**, *30* (44), 1800941.

(18) Inal, S.; Malliaras, G. G.; Rivnay, J. Benchmarking Organic Mixed Conductors for Transistors. *Nat. Commun.* **2017**, *8* (1), 1−6.

(19) Keene, S. T.; Pol, T. P. A.; Zakhidov, D.; Weijtens, C. H. L.; Janssen, R. A. J.; Salleo, A.; Burgt, Y. Enhancement-Mode PEDOT:PSS Organic Electrochemical Transistors Using Molecular De-Doping. *Adv. Mater.* **2020**, *32* (19), 2000270.

(20) Donahue, M. J.; Sanchez-Sanchez, A.; Inal, S.; Qu, J.; Owens, R. M.; Mecerreyes, D.; Malliaras, G. G.; Martin, D. C. Tailoring PEDOT Properties for Applications in Bioelectronics. *Materials Science and Engineering R: Reports*; Elsevier, 2020; p 100546.

(21) Huang, L.; Yang, X.; Deng, L.; Ying, D.; Lu, A.; Zhang, L.; Yu, A.; Duan, B. Biocompatible Chitin Hydrogel Incorporated with PEDOT Nanoparticles for Peripheral Nerve Repair. *ACS Appl. Mater. Interfaces* **2021**, *13* (14), 16106−16117.

(22) Zamora-Sequeira, R.; Ardao, I.; Starbird, R.; García-González, C. A. Conductive Nanostructured Materials Based on Poly-(3,4-Ethylenedioxythiophene) (PEDOT) and Starch/κ-Carrageenan for Biomedical Applications. *Carbohydr. Polym.* **2018**, *189*, 304−312.

(23) Wei, B.; Ouyang, L.; Liu, J.; Martin, D. C. Post-Polymerization Functionalization of Poly(3,4-Propylenedioxythiophene) (PProDOT) via Thiol-Ene "Click" Chemistry. *J. Mater. Chem. B* **2015**, *3* (25), 5028−5034.

(24) Povlich, L. K.; Cho, J. C.; Leach, M. K.; Corey, J. M.; Kim, J.; Martin, D. C. Synthesis, Copolymerization and Peptide-Modification of Carboxylic Acid-Functionalized 3,4-Ethylenedioxythiophene (EDOTacid) for Neural Electrode Interfaces. *Biochim. Biophys. Acta - Gen. Subj.* **2013**, *1830* (9), 4288−4293.

(25) Khau, B. V.; Savagian, L. R.; De Keersmaecker, M.; Gonzalez, M. A.; Reichmanis, E. Carboxylic Acid Functionalization Yields Solvent-Resistant Organic Electrochemical Transistors. *ACS Mater. Lett.* **2019**, *1* (6), 599−605.

(26) Hai, W.; Goda, T.; Takeuchi, H.; Yamaoka, S.; Horiguchi, Y.; Matsumoto, A.; Miyahara, Y. Human Influenza Virus Detection Using Sialyllactose-Functionalized Organic Electrochemical Transistors. *Sensors Actuators, B Chem.* **2018**, *260*, 635−641.

(27) Daprà, J.; Lauridsen, L. H.; Nielsen, A. T.; Rozlosnik, N. Comparative Study on Aptamers as Recognition Elements for Antibiotics in a Label-Free All-Polymer Biosensor. *Biosens. Bioelectron.* **2013**, *43* (1), 315−320.

(28) Ouyang, L.; Wei, B.; Kuo, C.-c.; Pathak, S.; Farrell, B.; Martin, D. C. Enhanced PEDOT Adhesion on Solid Substrates with Electrografted P(EDOT-NH2). *Sci. Adv.* **2017**, *3* (3), 1−12.

(29) Tropp, J.; Mehta, A. S.; Wu, R.; Reddy, M. M.; Patel, S. P.; Ii, A. J. P.; Rivnay, J. PEDOT-NHS as a Versatile Conjugated Polyelectrolyte for Bioelectronics. *ChemRxiv* **2022**, DOI: 10.26434/chemrxiv-2022-x8kdv.

(30) Wu, B.; Cao, B.; Taylor, I. M.; Woeppel, K.; Cui, X. T. Facile Synthesis of a 3,4-Ethylene-Dioxythiophene (EDOT) Derivative for Ease of Bio-Functionalization of the Conducting Polymer PEDOT. *Front. Chem.* **2019**, DOI: 10.3389/fchem.2019.00178.

(31) Istif, E.; Mantione, D.; Vallan, L.; Hadziioannou, G.; Brochon, C.; Cloutet, E.; Pavlopoulou, E. Thiophene-Based Aldehyde Derivatives for Functionalizable and Adhesive Semiconducting Polymers. *ACS Appl. Mater. Interfaces* **2020**, *12* (7), 8695−8703.

(32) Kaur, J.; Saxena, M.; Rishi, N. An Overview of Recent Advances in Biomedical Applications of Click Chemistry. *Bioconjugate Chem.* **2021**, *32* (8), 1455−1471.

(33) Yameen, B.; Ali, M.; Álvarez, M.; Neumann, R.; Ensinger, W.; Knoll, W.; Azzaroni, O. A Facile Route for the Preparation of Azide-Terminated Polymers. "Clicking" Polyelectrolyte Brushes on Planar Surfaces and Nanochannels. *Polym. Chem.* **2010**, *1* (2), 183−192.

(34) Moses, J. E.; Moorhouse, A. D.; Moses, J. E.; Sharpless, K. B. *Growing Applications of Click Chemistry* **2007**, *36*, 1249−1262.

(35) Fantoni, N. Z.; El-Sagheer, A. H.; Brown, T. A Hitchhiker's Guide to Click-Chemistry with Nucleic Acids. *Chem. Rev.* **2021**, *121* (12), 7122−7154.

(36) Xi, W.; Scott, T. F.; Kloxin, C. J.; Bowman, C. N. Click Chemistry in Materials Science. *Adv. Funct. Mater.* **2014**, *24* (18), 2572−2590.

(37) El-Sagheer, A. H.; Brown, T. Click Chemistry with DNA. *Chem. Soc. Rev.* **2010**, *39* (4), 1388−1405.

(38) Jewett, J. C.; Bertozzi, C. R. Cu-Free Click Cycloaddition Reactions in Chemical Biology. *Chem. Soc. Rev.* **2010**, *39* (4), 1272−1279.

(39) Shavokshina, V. A.; Komkova, M. A.; Aparin, I. O.; Zatsepin, T. S.; Karyakin, A. A.; Andreev, E. A. Improved Electroactivity of Redox Probes onto Electropolymerized Azidomethyl-PEDOT: Enabling Click Chemistry for Advanced (Bio)Sensors. *ACS Appl. Polym. Mater.* **2021**, *3* (3), 1518−1524.

(40) Yáñez-Sedeño, P.; González-Cortés, A.; Campuzano, S.; Pingarrón, J. M. Copper(I)-Catalyzed Click Chemistry as a Tool for the Functionalization of Nanomaterials and the Preparation of Electrochemical (Bio)Sensors. *Sensors* **2019**, *19* (10), 2379.

(41) Godeau, G.; N'Na, J.; Darmanin, T.; Guittard, F. Azidomethyl-EDOT as a Platform for Tunable Surfaces with Nanostructures and Superhydrophobic Properties. *J. Phys. Chem. B* **2015**, *119* (22), 6873−6877.

(42) Bu, H. B.; Götz, G.; Reinold, E.; Vogt, A.; Schmid, S.; Blanco, R.; Segura, J. L.; Bäuerle, P. Click"-Functionalization of Conducting Poly(3,4- Ethylenedioxythiophene) (PEDOT). *Chem. Commun.* **2008**, No. 11, 1320−1322.

(43) Daugaard, A. E.; Hvilsted, S.; Hansen, T. S.; Larsen, N. B. Conductive Polymer Functionalization by Click Chemistry. *Macromolecules* **2008**, *41* (12), 4321−4327.

(44) Marrocchi, A.; Facchetti, A.; Lanari, D.; Santoro, S.; Vaccaro, L. Click-Chemistry Approaches to π-Conjugated Polymers for Organic Electronics Applications. *Chem. Sci.* **2016**, *7* (10), 6298−6308.

(45) Wang, J. T.; Takshima, S.; Wu, H. C.; Shih, C. C.; Isono, T.; Kakuchi, T.; Satoh, T.; Chen, W. C. Stretchable Conjugated Rod-Coil Poly(3-Hexylthiophene)-Block-Poly(Butyl Acrylate) Thin Films for Field Effect Transistor Applications. *Macromolecules* **2017**, *50* (4), 1442−1452.

(46) Paoprasert, P.; Spalenka, J. W.; Peterson, D. L.; Ruther, R. E.; Hamers, R. J.; Evans, P. G.; Gopalan, P. Grafting of Poly(3-Hexylthiophene) Brushes on Oxides Using Click Chemistry. *J. Mater. Chem.* **2010**, *20* (13), 2651−2658.

(47) Freudenberg, J.; Jänsch, D.; Hinkel, F.; Bunz, U. H. F. Immobilization Strategies for Organic Semiconducting Conjugated Polymers. *Chem. Rev.* **2018**, *118* (11), 5598−5689.

(48) Mishyn, V.; Rodrigues, T.; Leroux, Y. R.; Aspermair, P.; Happy, H.; Bintinger, J.; Kleber, C.; Boukherroub, R.; Knoll, W.; Szunerits, S. Controlled Covalent Functionalization of a Graphene-Channel of a Field Effect Transistor as an Ideal Platform for (Bio)Sensing Applications. *Nanoscale Horiz.* **2021**, *6* (10), 819−829.

(49) Li, N.; Dai, Y.; Li, Y.; Dai, S.; Strzalka, J.; Su, Q.; De Oliveira, N.; Zhang, Q.; St. Onge, P. B. J.; Rondeau-Gagné, S.; Wang, Y.; Gu, X.; Xu, J.; Wang, S. A Universal and Facile Approach for Building Multifunctional Conjugated Polymers for Human-Integrated Electronics. *Matter* **2021**, *4* (9), 3015−3029.

(50) Segura, J. L.; Gómez, R.; Reinold, E.; Bäuerle, P. Synthesis and Electropolymerization of a Perylenebisimide-Functionalized 3,4-Ethylenedioxythiophene (EDOT) Derivative. *Org. Lett.* **2005**, *7* (12), 2345−2348.

(51) Segura, J. L.; Gómez, R.; Blanco, R.; Reinold, E.; Bäuerle, P. Synthesis and Electronic Properties of Anthraquinone-, Tetracyanoanthraquinodimethane-, and Perylenetetracarboxylic Diimide-Functionalized Poly(3,4-Ethylenedioxythiophenes). *Chem. Mater.* **2006**, *18* (12), 2834−2847.

(52) Musumeci, C.; Hutchison, J. A.; Samorì, P. Controlling the Morphology of Conductive PEDOT by in Situ Electropolymerization: From Thin Films to Nanowires with Variable Electrical Properties. *Nanoscale* **2013**, *5* (17), 7756−7761.

(53) Travaglini, L.; Micolich, A. P.; Cazorla, C.; Zeglio, E.; Lauto, A.; Mawad, D. Single-Material OECT-Based Flexible Complementary Circuits Featuring Polyaniline in Both Conducting Channels. *Adv. Funct. Mater.* **2021**, *31* (4), 2007205.

(54) Gu, M.; Travaglini, L.; Hopkins, J.; Ta, D.; Lauto, A.; Wagner, P.; Wagner, K.; Zeglio, E.; Jephcott, L.; Officer, D. L.; Mawad, D. Molecular Design of an Electropolymerized Copolymer with Carboxylic and Sulfonic Acid Functionalities. *Synth. Met.* **2022**, *285* (December), 117029.

(55) Fan, J.; Rezaie, S. S.; Facchini-Rakovich, M.; Gudi, D.; Montemagno, C.; Gupta, M. Tuning PEDOT:PSS Conductivity to Obtain Complementary Organic Electrochemical Transistor. *Org. Electron. physics, Mater. Appl.* **2019**, *66* (October), 148−155.

(56) Fenoy, G. E.; Marmisollé, W. A.; Azzaroni, O.; Knoll, W. Acetylcholine Biosensor Based on the Electrochemical Functionalization of Graphene Field-Effect Transistors. *Biosens. Bioelectron.* **2020**, *148*, 111796.

(57) Rivnay, J.; Leleux, P.; Sessolo, M.; Khodagholy, D.; Hervé, T.; Fiocchi, M.; Malliaras, G. G. Organic Electrochemical Transistors with Maximum Transconductance at Zero Gate Bias. *Adv. Mater.* **2013**, *25* (48), 7010−7014.

(58) Yu, S.; Ratcliff, E. L. Tuning Organic Electrochemical Transistor (OECT) Transconductance toward Zero Gate Voltage in the Faradaic Mode. *ACS Appl. Mater. Interfaces* **2021**, *13* (42), 50176−50186.

(59) Ko, Y. H.; Kim, Y. H.; Park, J.; Nam, K. T.; Park, J. H.; Yoo, P. J. Electric-Field-Assisted Layer-by-Layer Assembly of Weakly Charged Polyelectrolyte Multilayers. *Macromolecules* **2011**, *44* (8), 2866−2872.

(60) Shavokshina, V. A.; Komkova, M. A.; Aparin, I. O.; Zatsepin, T. S.; Karyakin, A. A.; Andreev, E. A. Improved Electroactivity of Redox Probes onto Electropolymerized Azidomethyl-PEDOT: Enabling Click Chemistry for Advanced (Bio)Sensors. *ACS Appl. Polym. Mater.* **2021**, *3* (3), 1518−1524.

(61) Luo, S. C.; Ali, E. M.; Tansil, N. C.; Yu, H. H.; Gao, S.; Kantchev, E. A. B.; Ying, J. Y. Poly(3,4-Ethylenedioxythiophene) (PEDOT) Nanobiointerfaces: Thin, Ultrasmooth, and Functionalized PEDOT Films with in Vitro and in Vivo Biocompatibility. *Langmuir* **2008**, *24* (15), 8071−8077.

(62) Hui, Y.; Bian, C.; Xia, S.; Tong, J.; Wang, J. Synthesis and Electrochemical Sensing Application of Poly(3,4-Ethylenedioxythiophene)-Based Materials: A Review. *Anal. Chim. Acta* **2018**, *1022*, 1−19.

(63) Khodagholy, D.; Rivnay, J.; Sessolo, M.; Gurfinkel, M.; Leleux, P.; Jimison, L. H.; Stavrinidou, E.; Herve, T.; Sanaur, S.; Owens, R. M.; Malliaras, G. G. High Transconductance Organic Electrochemical Transistors. *Nat. Commun.* **2013**, *4*, 1−6.

(64) Savva, A.; Hallani, R.; Cendra, C.; Surgailis, J.; Hidalgo, T. C.; Wustoni, S.; Sheelamanthula, R.; Chen, X.; Kirkus, M.; Giovannitti, A.; Salleo, A.; McCulloch, I.; Inal, S. Balancing Ionic and Electronic Conduction for High-Performance Organic Electrochemical Transistors. *Adv. Funct. Mater.* **2020**, *30* (11), 1907657.

(65) Faria, G. C.; Duong, D. T.; Salleo, A. On the Transient Response of Organic Electrochemical Transistors. *Org. Electron.* **2017**, *45*, 215−221.

(66) Bernards, D. A.; Malliaras, G. G. Steady-State and Transient Behavior of Organic Electrochemical Transistors. *Adv. Funct. Mater.* **2007**, *17* (17), 3538−3544.

(67) Zeglio, E.; Vagin, M.; Musumeci, C.; Ajjan, F. N.; Gabrielsson, R.; Trinh, X. T.; Son, N. T.; Maziz, A.; Solin, N.; Inganäs, O. Conjugated Polyelectrolyte Blends for Electrochromic and Electrochemical Transistor Devices. *Chem. Mater.* **2015**, *27* (18), 6385−6393.

(68) Horowitz, G. Organic Field-Effect Transistors. *Adv. Mater.* **1998**, *10* (5), 365−377.

(69) Hopkins, J.; Fidanovski, K.; Travaglini, L.; Ta, D.; Hook, J.; Wagner, P.; Wagner, K.; Lauto, A.; Cazorla, C.; Officer, D.; Mawad, D. A Phosphonated Poly(Ethylenedioxythiophene) Derivative with Low Oxidation Potential for Energy-Efficient Bioelectronic Devices. *Chem. Mater.* **2022**, *34* (1), 140−151.

(70) Fan, J.; Rezaie, S. S.; Facchini-Rakovich, M.; Gudi, D.; Montemagno, C.; Gupta, M. Tuning PEDOT:PSS Conductivity to Obtain Complementary Organic Electrochemical Transistor. *Org. Electron.* **2019**, *66*, 148−155.

(71) Fenoy, G. E.; Giussi, J. M.; von Bilderling, C.; Maza, E. M.; Pietrasanta, L. I.; Knoll, W.; Marmisollé, W. A.; Azzaroni, O. Reversible Modulation of the Redox Activity in Conducting Polymer Nanofilms Induced by Hydrophobic Collapse of a Surface-Grafted Polyelectrolyte. *J. Colloid Interface Sci.* **2018**, *518*, 92−101.

(72) Pecqueur, S.; Lončarić, I.; Zlatić, V.; Vuillaume, D.; Crljen, Ž. The Non-Ideal Organic Electrochemical Transistors Impedance. *Org. Electron.* **2019**, *71* (January), 14−23.

(73) Volkov, A. V.; Wijeratne, K.; Mitraka, E.; Ail, U.; Zhao, D.; Tybrandt, K.; Andreasen, J. W.; Berggren, M.; Crispin, X.; Zozoulenko, I. V. Understanding the Capacitance of PEDOT:PSS. *Adv. Funct. Mater.* **2017**, *27* (28), 1700329.

(74) Rivnay, J.; Inal, S.; Collins, B. A.; Sessolo, M.; Stavrinidou, E.; Strakosas, X.; Tassone, C.; Delongchamp, D. M.; Malliaras, G. G. Structural Control of Mixed Ionic and Electronic Transport in Conducting Polymers. *Nat. Commun.* **2016**, *7*, 1−9.

(75) Nielsen, C. B.; Giovannitti, A.; Sbircea, D. T.; Bandiello, E.; Niazi, M. R.; Hanifi, D. A.; Sessolo, M.; Amassian, A.; Malliaras, G. G.; Rivnay, J.; McCulloch, I. Molecular Design of Semiconducting Polymers for High-Performance Organic Electrochemical Transistors. *J. Am. Chem. Soc.* **2016**, *138* (32), 10252−10259.

(76) Lind, J. U.; Hansen, T. S.; Daugaard, A. E.; Hvilsted, S.; Andresen, T. L.; Larsen, N. B. Solvent Composition Directing Click-Functionalization at the Surface or in the Bulk of Azide-Modified PEDOT. *Macromolecules* **2011**, *44* (3), 495−501.

(77) Doris, S. E.; Pierre, A.; Street, R. A. Dynamic and Tunable Threshold Voltage in Organic Electrochemical Transistors. *Adv. Mater.* **2018**, *30* (15), 1706757.

(78) Hansen, T. S.; Daugaard, A. E.; Hvilsted, S.; Larsen, N. B. Spatially Selective Functionalization of Conducting Polymers by "Electroclick" Chemistry. *Adv. Mater.* **2009**, *21* (44), 4483−4486.

(79) Bu, H. B.; Götz, G.; Reinold, E.; Vogt, A.; Schmid, S.; Segura, J. L.; Blanco, R.; Gómez, R.; Bäuerle, P. Efficient Post-Polymerization Functionalization of Conducting Poly(3,4-Ethylenedioxythiophene) (PEDOT) via 'Click'-Reaction. *Tetrahedron* **2011**, *67* (6), 1114−1125.

(80) Wayment, J. R.; Harris, J. M. Biotin-Avidin Binding Kinetics Measured by Single-Molecule Imaging. *Anal. Chem.* **2009**, *81* (1), 336−342.

(81) Baba, A.; Lübben, J.; Tamada, K.; Knoll, W. Optical Properties of Ultrathin Poly(3,4-Ethylenedioxythiophene) Films at Several Doping Levels Studied by In Situ Electrochemical Surface Plasmon Resonance Spectroscopy. *Langmuir* **2003**, *19* (21), 9058−9064.

(82) Linman, M. J.; Taylor, J. D.; Yu, H.; Chen, X.; Cheng, Q. Surface Plasmon Resonance Study of Protein-Carbohydrate Interactions Using Biotinylated Sialosides. *Anal. Chem.* **2008**, *80* (11), 4007−4013.

(83) Orelma, H.; Johansson, L. S.; Filpponen, I.; Rojas, O. J.; Laine, J. Generic Method for Attaching Biomolecules via Avidin-Biotin Complexes Immobilized on Films of Regenerated and Nanofibrillar Cellulose. *Biomacromolecules* **2012**, *13* (9), 2802−2810.

(84) Bartlett, P. N.; Birkin, P. R.; Palmisano, F.; De Benedetto, G. A Study on the Direct Electrochemical Communication between Horseradish Peroxidase and a Poly(Aniline) Modified Electrode. *J. Chem. Soc. Faraday Trans.* **1996**, *92* (17), 3123.

(85) Ferri, T.; Poscia, A.; Santucci, R. Direct Electrochemistry of Membrane-Entrapped Horseradish Peroxidase. Part II: Amperometric Detection of Hydrogen Peroxide. *Bioelectrochemistry Bioenerg.* **1998**, *45* (2), 221−226.

(86) Derszniak, K.; Przyborowski, K.; Matyjaszczyk, K.; Moorlag, M.; de Laat, B.; Nowakowska, M.; Chlopicki, S. Comparison of Effects of Anti-Thrombin Aptamers HD1 and HD22 on Aggregation of Human Platelets, Thrombin Generation, Fibrin Formation, and Thrombus Formation Under Flow Conditions. *Front. Pharmacol.* **2019**, *10* (FEB), 1−13.

(87) Crawley, J. T. B.; Zanardelli, S.; Chion, C. K. N. K.; Lane, D. A. The Central Role of Thrombin in Hemostasis. *J. Thromb. Haemost.* **2007**, *5* (Suppl 1), 95−101.

(88) Kotlarek, D.; Curti, F.; Vorobii, M.; Corradini, R.; Careri, M.; Knoll, W.; Rodriguez-Emmenegger, C.; Dostálek, J. Surface Plasmon Resonance-Based Aptasensor for Direct Monitoring of Thrombin in a Minimally Processed Human Blood. *Sensors Actuators, B Chem.* **2020**, *320* (February), 128380.

(89) Kotlarek, D.; Curti, F.; Vorobii, M.; Corradini, R.; Careri, M.; Knoll, W.; Rodriguez-Emmenegger, C.; Dostálek, J. Surface Plasmon Resonance-Based Aptasensor for Direct Monitoring of Thrombin in a Minimally Processed Human Blood. *Sensors Actuators, B Chem.* **2020**, *320* (June), 128380.

(90) Hasler, R.; Reiner-Rozman, C.; Fossati, S.; Aspermair, P.; Dostalek, J.; Lee, S.; Ibáñez, M.; Bintinger, J.; Knoll, W. Field-Effect Transistor with a Plasmonic Fiber Optic Gate Electrode as a Multivariable Biosensor Device. *ACS Sensors* **2022**, *7* (2), 504−512.

(91) Hammock, M. L.; Knopfmacher, O.; Naab, B. D.; Tok, J. B. H.; Bao, Z. Investigation of Protein Detection Parameters Using Nanofunctionalized Organic Field-Effect Transistors. *ACS Nano* **2013**, *7* (5), 3970−3980.

(92) Lin, P. H.; Chen, R. H.; Lee, C. H.; Chang, Y.; Chen, C. S.; Chen, W. Y. Studies of the Binding Mechanism between Aptamers and Thrombin by Circular Dichroism, Surface Plasmon Resonance and Isothermal Titration Calorimetry. *Colloids Surfaces B Biointerfaces* **2011**, *88* (2), 552−558.

(93) Hong, V.; Presolski, S. I.; Ma, C.; Finn, M. G. Analysis and Optimization of Copper-Catalyzed Azide−Alkyne Cycloaddition for Bioconjugation. *Angew. Chemie Int. Ed.* **2009**, *48* (52), 9879−9883.